PAPER

NJC
www.rsc.org/njc

Structural, spectroscopic and computational studies of the HgL_2Cl_2 complex (L = 3,5-dimethyl-1-thiocarboxamide pyrazole) and the crystal structure of L†

Attila Kovács,*[a] Dénes Nemcsok,[a] György Pokol,[b] Katalin Mészáros Szécsényi,*[c] Vukadin M. Leovac,[c] Željko K. Jaćimović,[d] Ivana Radosavljević Evans,[e] Judith A. K. Howard,[e] Zoran D. Tomić[f] and Gerald Giester[g]

[a] *Research Group of Technical Analytical Chemistry, Hungarian Academy of Sciences, Budapest University of Technology and Economics, Szt. Gellért tér 4, H-1111 Budapest, Hungary. E-mail: akovacs@mail.bme.hu; Fax: +361 463 3408; Tel: +361 463 2278*

[b] *Institute of General and Analytical Chemistry, Budapest University of Technology and Economics, Szt. Gellért tér 4, H-1111 Budapest, Hungary*

[c] *Department of Chemistry, Faculty of Sciences, University of Novi Sad, Trg D. Obradovića 3, 21000 Novi Sad, Serbia and MontenegroE-mail: mszk@im.ns.ac.yu; Fax: +381 21 454 065; Tel: +381 21 350 672*

[d] *Faculty of Metallurgy and Technology, University of Montenegro, 8100 Podgorica, Serbia and Montenegro*

[e] *Department of Chemistry, University of Durham, Science Site, South Road, Durham, DH1 3LE, England*

[f] *Institute of Nuclear Sciences "Vinča", P. O. Box 522, 11001 Belgrade, Serbia and Montenegro*

[g] *Institut für Mineralogie und Kristallographie, Universität Wien, Althanstraße 14, A-1090 Vienna, Austria*

Received (in Montpellier, France) 2nd November 2004, Accepted 11th March 2005
First published as an Advance Article on the web 5th May 2005

In the present paper we report the synthesis as well as the structural and vibrational characterisation of the HgL_2Cl_2 complex (L = 3,5-dimethyl-1-thiocarboxamide). The crystal and molecular structures of both L and the HgL_2Cl_2 complex were determined by single-crystal X-ray diffraction. The coordination propensity of L to $HgCl_2$ was explored by quantum chemical calculations. We found the preference of the monodentate coordination of L to $HgCl_2$ through the sulfur atom (instead of the "pyridine" nitrogen) to be in agreement with Pearson's acid–base character of the atoms involved and the steric effects. The vibrational properties of HgL_2Cl_2 were evaluated by a joint FT-IR and quantum chemical analysis. In addition, the thermal decomposition of the complex and ligand is reported.

1. Introduction

Pyrazole type compounds and their complexes are of great interest in chemical research due to their biological activity.[2] Pyrazole based ligands have been proposed as model compounds for active sites in metalloproteins.[3] These proteins like tyrosinase have both catacholase and cresolase activity.[4] As enzymatic syntheses have often been conducted under mild conditions and are very selective, they can be used as models to study biocatalytic mechanisms with potential applications in chemical industry. Gamez *et al.* synthesised a complex of Cu(II) with 1,3-bis(3,5-dimethylpyrazol-1-yl)-propan-2-ol and investigated its ability to catalyse the oxidative coupling of 2,6-dimethylphenol as a biomimetic dinuclear catalyst in order to obtain poly(1,4-ethylene ether).[5]

In recent years, metal complexes with pyrazole type ligands have been introduced as precursors in metal organic vapour deposition (MOCVD) processes.[6–8] The chemistry and the reactions of pyrazole type complexes have been described in detail in several review articles.[9–12]

Our systematic studies of transition metal complexes with pyrazole derivatives[13–16] have the aim to synthesise new compounds with structural properties that fulfil the specific stereochemical requirements of a particular metal-binding site and to determine the conditions of complex formation in order to understand the factors governing reaction pathways. Studies of the crystal structures of the ligands and their complexes can give valuable information about the factors determining the course of complex formation. In addition, analysis of the thermal decomposition of the complexes offers insight into possible ways to synthesise new compounds in the solid state.

In our previous publications[17–19] we presented the synthesis and structural characterisation of Ni(II), Cu(I,II), Co(II) and Co(III) complexes with 3,5-dimethyl-1-thiocarboxamide pyrazole (**L**). In the present study, we investigated the coordination properties of the sulfur-donor ligand **L** to Hg(II). This is an important subject, as mercury is a highly toxic element and its transport and accumulation in living organisms is mainly due to interactions with the sulfur atoms in proteins.[20]

In this paper we describe the synthesis, physico-chemical properties and the crystal structure of **L** and its complex with $HgCl_2$. We present the vibrational analysis of HgL_2Cl_2 on the basis of FT-IR experiments and quantum chemical calcula-

† This paper is Part 20 in the series of our studies on Transition Metal Complexes with pyrazole based ligands. Part 19.[1]

DOI: 10.1039/b416816j

tions. Using theoretical calculations, we investigate the bonding interactions between **L** and $HgCl_2$, probing different possible coordination modes. The course of complex formation is discussed on the basis of the Pearson basicity of the interacting atoms and the steric hindrance of the substituents. In addition, we report the thermal decomposition of the ligand and HgL_2Cl_2.

2. Experimental

2.1. General

All chemicals were reagent grade, commercially available, and were used without any purification.

The FT-IR spectra of HgL_2Cl_2 were obtained from KBr and polyethylene pellets in the mid-IR (4000–450 cm^{-1}) and far-IR (650–150 cm^{-1}) ranges. The measurements were performed at room temperature on a Perkin Elmer System 2000 FT-IR spectrometer operating with MCT detector in the mid-IR (16 scans) and DTGS detector in the far-IR (64 scans) ranges. The resolution was 4 cm^{-1}.

The thermal analyses were carried out in argon and air atmospheres using a DuPont 2000 TA system with a thermobalance DuPont 951 TGA. During the thermogravimetric measurements the samples were heated in a platinum crucible with a heating rate of 10 K min^{-1} up to 1000 K. The DSC curves were recorded with the same heating rate up to 600 K using an open aluminium pan as sample holder and an empty pan as reference. The molar conductivity of a freshly prepared 10^{-3} mol dm^{-3} solution of HgL_2Cl_2 in DMF was measured at room temperature using a Jenway 4010 conductivity meter. The carbon, hydrogen and nitrogen contents were determined by standard analytical methods.

2.2. Syntheses

2.2.1. 3,5-Dimethyl-1-thiocarboxamide (L). **L** was prepared by the reaction of thiosemicarbazide (tsc) and 2,4-pentandione (Hacac) in a mole ratio of 1 : 1. Five grams of tsc was dissolved in 250 cm^3 cold water with addition of 1 cm^3 conc. HCl. The solution was filtered and 5 cm^3 Hacac was added to the filtrate. The mixture was stirred with a magnetic stirrer for 30 min and left to stand for 6 h. The white precipitate was filtered off, washed with cold water and dried in air. Yield: 6.8 g (80.0%). Single crystals for the structure determination were grown in acetonic solution but can also be obtained by recrystallisation from ethyl ether. Anal found (calcd) %: C 46.18 (46.43); H 5.67 (5.84); N 27.07 (26.92).

2.2.2. HgL_2Cl_2. $HgCl_2$ (0.27 g, 1 mmol) was dissolved in 5 cm^3 cold methanol and was mixed with the solution of 0.31 g (2 mmol) **L** in 5 cm^3 methanol. After 2 h the white precipitate was filtered off, washed with cold methanol and dried in air. Yield: 0.35 g (45.2%). λ_M: 7.5 S cm^2 mol^{-1} (DMF). The reaction was also carried out with an $HgCl_2$ to **L** mole ratio of 1 : 1, but the same product was obtained. Anal. found (calcd) %: C 24.63 (24.75), H 3.13 (3.12), N 14.61 (14.43).

2.3. X-Ray crystallography‡

A crystal of **L** with approximate dimensions of 0.42 × 0.36 × 0.22 mm^3 was measured at 150 K on a Nonius Kappa CCD diffractometer equipped with an Oxford Cryosystems cooling system and using MoK_α radiation. The data collection was performed using a 2° rotation width of the 368 frames (60 s exposure time per frame).

The structure was solved by direct methods using SIR92[21] and refined by a full-matrix least-squares method based on F^2, including all reflections. All non-hydrogen atoms were refined anisotropically using SHELXL-97.[22] Hydrogen atoms were positioned geometrically at calculated positions and allowed to ride on their parent atoms. The refinement converged to R = 3.97%, and wR = 10.38%. The maximum and minimum residual electron densities in the final ΔF map were 0.753 and −0.654 e $Å^{-3}$, respectively. The largest residual electron density peak is at 1.16 Å from the hydrogen atom H_2. The geometrical analysis was performed using PLATON-99.[23]

A single crystal of HgL_2Cl_2 with approximate dimensions of 0.04 × 0.08 × 0.30 mm^3 was selected for data collection. The data were collected at 120 K on a Bruker AXS SMART diffractometer with an APEX CCD detector, equipped with a Bede Microsource® X-ray generator and an Oxford Cryosystems N_2 cryostream cooling system, using Mo K_α radiation. A full sphere of data was collected with a frame width of 0.3° and a counting time of 30 s per frame. Data reduction was carried out using the SAINT[24] software suite. A multiscan absorption correction[25] was applied to the raw data and the resulting R_{int} was 3.1%. The crystal structure was solved by direct methods using SIR92[21] and refined using the Crystals[26] software package. Hydrogen atoms were placed geometrically and treated using a riding model. A full-matrix least-squares refinement against F^2 converged to the agreement factors of R = 2.68% and wR = 6.94%. The maximum and minimum residual electron densities were 2.09 and −1.93 e $Å^{-3}$, respectively; the largest residual electron density peaks are within 0.8 Å of the heavy Hg atom. Selected crystallographic details are given in Table 1.

2.4. Computational details

The quantum chemical calculations were carried out with the GAUSSIAN 98 program package[27] using the Becke3–Lee–Yang–Parr (B3-LYP)[28,29] exchange–correlation functional. The relativistic effective core potential and its [21/21/21] valence basis set of Hay and Wadt[30] was used for Hg, extended by a single set of f-type polarisation functions (α = 1.002).[31] The 6-31G** basis set was applied for H, C, O, Cl and S. The character (minimum or saddle point) of the optimised

Table 1 Crystal data for **L** and HgL_2Cl_2

	L	HgL_2Cl_2
Chemical formula	$C_6N_3SH_9$	$[Hg(C_6N_3SH_9)_2Cl_2]$
Molecular weight	155.22	581.94
Crystal system	Triclinic	Triclinic
Space group	$P\bar{1}$	$P\bar{1}$
a/Å	8.413(2)	8.820(1)
b/Å	9.333(2)	9.920(2)
c/Å	10.846(2)	11.133(2)
α/°	68.71(3)	82.063(3)
β/°	73.31(3)	80.698(3)
γ/°	76.70(3)	83.015(3)
U/$Å^3$	752.5(3)	947.1(3)
Z	4	2
T/K	140	120
Calcd density/g cm^{-3}	1.370	2.040
μ/mm^{-1}	0.354	8.634
Total number of reflections	6836	12 512
Number of unique reflections	3698	5533
Number of observed reflections ($I > 2\sigma$)	2850	5171
Number of parameters refined	185	208
Data-to-parameter ratio	20	25
R_{int} (%)	2.4	3.1
R (%) for $I > 2\sigma$	3.97	2.68
wR (%) for all reflections	10.38	6.96

‡ CCDC reference numbers 266480 and 266481. See http://www.rsc.org/suppdata/nj/b4/b416816j/ for crystallographic data in CIF or other electronic format.

Table 2 Bond lengths (Å) and angles (°) in the ligand molecules (**L** and L′)

N1–N2	1.389(3)	N11–N12	1.390(3)
N1–C3	1.394(3)	N11–C13	1.395(3)
N1–C4	1.403(3)	N11–C14	1.405(3)
N2–C1	1.324(3)	N12–C11	1.322(3)
N3–C4	1.325(3)	N13–C14	1.315(3)
C2–C1	1.415(4)	C12–C11	1.411(4)
C2–C3	1.356(4)	C12–C13	1.360(4)
C5–C1	1.498(4)	C15–C11	1.493(3)
C6–C3	1.489(4)	C16–C13	1.490(4)
S1–C4	1.660(3)	S11–C14	1.673(3)
N2–N1–C3	111.1(2)	N12–N11–C13	111.4(2)
N2–N1–C4	118.2(2)	N12–N11–C14	117.9(2)
C3–N1–C4	130.8(2)	C13–N11–C14	130.7(2)
C1–N2–N1	104.9(2)	C11–N12–N11	104.8(2)
N3–C4–N1	113.6(2)	N13–C14–N11	114.8(2)
N3–C4–S1	122.7(2)	N13–C14–S11	123.2(2)
N1–C4–S1	123.6(2)	N11–C14–S11	122.0(2)
C3–C2–C1	107.2(2)	C13–C12–C11	107.7(2)
N2–C1–C2	105.7(2)	N12–C11–C12	105.0(2)
N2–C1–C5	127.4(2)	N12–C11–C15	127.7(2)
C2–C1–C5	126.9(2)	C12–C11–C15	127.2(2)
C2–C3–N1	111.2(2)	C12–C13–N11	111.1(2)
C2–C3–C6	122.0(2)	C12–C13–C16	122.0(2)
N1–C3–C6	126.8(2)	N11–C13–C16	126.9(2)

structures was verified by frequency calculations. The relative stabilities of the different structures were evaluated from the computed absolute energies after zero-point vibrational energy (ZPE) corrections. The dissociation energy given in the paper includes additionally a correction for basis set superposition error (BSSE) estimated by the counterpoise method.[32]

3. Results and discussion

Both the ligand and the complex are white crystalline substances at room temperature. **L** is easily soluble in MeOH, EtOH, Me_2CO, DMF and DMSO, whereas only slightly soluble in water. The solubility of the complex is low in common solvents, but fairly good in DMF and DMSO. The low molar conductivity of HgL_2Cl_2 in DMF reflects its non-electrolytic character, similar to that of $HgCl_2$.

3.1. Crystal structure of L

The asymmetric unit contains two independent molecules of the ligand (designated as **L** and **L**′), but there are no significant differences in their geometric parameters (*cf.* Table 2). The molecular scheme and numbering of atoms for the molecule **L** are given in Fig. 1, while for **L**′ the corresponding atoms are numbered analogously using S11, C11, C12, *etc.*

A characteristic feature of the molecular geometry of **L** is the delocalisation of electrons within the pyrazole ring with a more pronounced double bond character of N2–C1 and C2–C3. The weak hydrogen bond between one of the amino hydrogens and N2 results in the anti orientation of S1 with respect to N2, as found previously in related pyrazolecarboxamides by ^{1}H NMR spectrometry.[33] Compared to the pyrazole parent,[34] the ring in **L** (**L**′) is somewhat expanded, as indicated by the longer bonds. The pyrazole ring is nearly planar: the largest deviation from the mean plane of the ring is 0.006(3) Å for atoms C3 and C13. The mean planes of the thiocarboxamide substituent (C4, S1, N3 and C14, S11, N13) and that of the corresponding ring form dihedral angles of 8.3(1)° and 11.5(2)° for molecules **L** and **L**′, respectively.

The packing of the molecules is determined by the intermolecular hydrogen bonds between the thiocarboxamide groups (Fig. 2). The molecules form hydrogen-bonded $R_2^2(8)$ centrosymmetric dimer units[35] with parameters H12···S11^i = 2.57 Å, N13–H12···S11^i = 166° (i = 2 − x, 2 − y, −z). Two additional molecules are connected to each dimer by S···H hydrogen bonds (H3···S1^{ii} = 2.49 Å, N3–H3···S1^i = 174°; ii = 1 − x, 1 − y, −z,). The torsion angle defined by N11–C14–S11–N3^{iii} is 57.90° (iii = x, +y, +z + 1), which means that the latter two molecules lie outside (approximately above and below) the plane of the dimer. These four-molecule units are mutually connected by stacking interactions between the neighbouring rings, thus forming chains along the c axis. The two closest rings involved in stacking contacts are parallel and the distance between the respective centroids is 3.70 Å. A partial overlap of the two rings is indicated by the angle of 22.6° between the normal to the ring and the line, which connects two centroids.

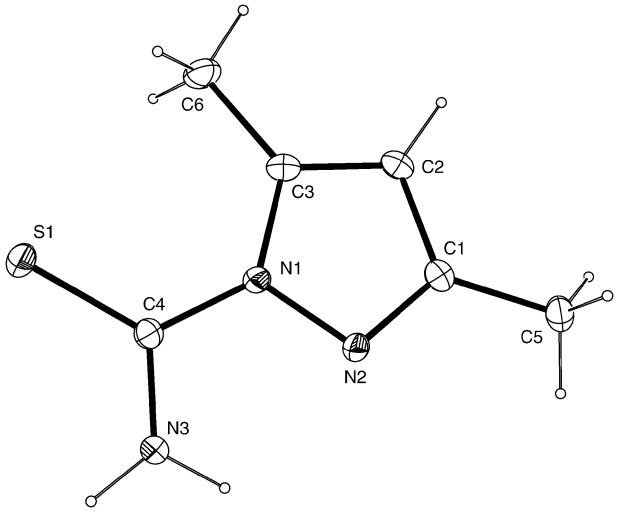

Fig. 1 Molecular diagram and atom numbering scheme of **L**; atomic displacement parameters are drawn at 50% probability level.

3.2. Crystal structure of HgL_2Cl_2

The molecular structure of the HgL_2Cl_2 complex with the atom numbering scheme is shown in Fig. 3. Selected bond lengths and angles are given in Table 3, together with the corresponding data obtained from the quantum chemical calculations. The Hg atom is in a distorted tetrahedral coordination, bonded to two Cl and two S atoms with angles ranging between 94° and 121°. The molecule contains an intramolecular hydrogen bond formed between the apical chlorine atom Cl11 and

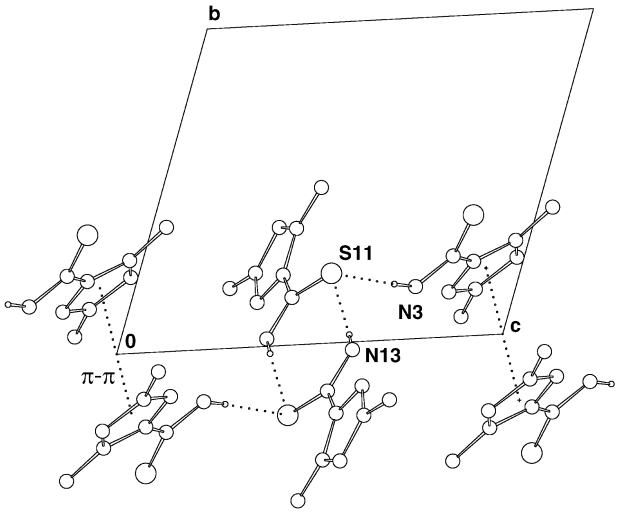

Fig. 2 Part of the unit cell showing the pattern of hydrogen bonding in **L**.

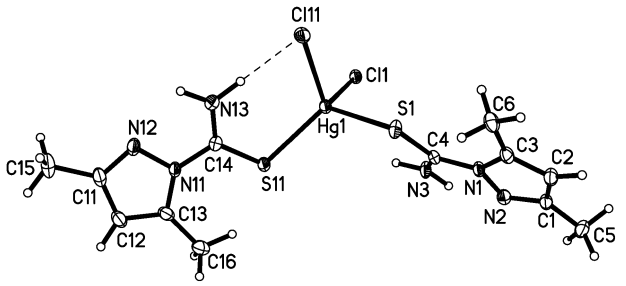

Fig. 3 Molecular diagram and atom numbering scheme for HgL_2Cl_2; atomic displacement parameters are drawn at 50% probability level.

hydrogen atom H17 of the amine group, with a Cl11···H17 distance of 2.19 Å and a Cl11···H17–N13 angle of 177°. The other NH_2 group is not involved in hydrogen bonding, as the Cl1···H7 distance is 3.06 Å. As a result of the single Cl···H hydrogen bond in HgL_2Cl_2, the molecular geometry in the crystal is asymmetric and this is also reflected in the slightly different geometrical parameters of the two ligands (*cf.* Table 3). Whereas most bond distances of the two ligand moieties

Table 3 Selected geometric parameters (Å, degrees) of HgL_2Cl_2 from the X-ray diffraction analysis and B3LYP/6-31G** calculations[a]

	Experimental		
	L	**L′**	Computed
Hg–Cl	2.4858(7)	2.5344(8)	2.544
Hg–S	2.5750(8)	2.4857(8)	2.831
S1–C4	1.690(3)	1.713(3)	1.703
C4–N3	1.314(3)	1.302(4)	1.322
C4–N1	1.391(3)	1.392(4)	1.414
N1–N2	1.391(3)	1.383(3)	1.381
N2–C1	1.312(4)	1.321(4)	1.319
N1–C3	1.399(3)	1.389(4)	1.397
C1–C2	1.431(4)	1.424(5)	1.424
C2–C3	1.365(4)	1.363(4)	1.372
C1–C5	1.493(4)	1.485(4)	1.496
C3–C6	1.490(4)	1.491(4)	1.494
Cl···H		2.187(3)	2.197
S1–Hg–S11	113.43(3)		102.0
S1–Hg–Cl11	107.75(2)		105.1
S11–Hg–Cl11	120.97(3)		102.1
S1–Hg–Cl1	94.14(3)		102.1
S11–Hg–Cl1	111.44(2)		105.1
Cl1–Hg–Cl11	105.58(3)		136.2
Hg–S1–C4	110.06(9)	108.02(10)	110.6
S1–C4–N1	120.5 (2)	119.1(2)	121.3
S1–C4–N3	124.7(2)	125.5(2)	124.9
N1–C4–N3	114.7(2)	115.4(2)	113.8
C4–N1–N2	115.9(2)	115.9(2)	116.4
C4–N1–C3	132.4(2)	132.4(2)	132.4
N2–N1–C3	111.5(2)	111.6(2)	111.2
N1–N2–C1	105.2(2)	105.3(3)	105.8
N2–C1–C2	111.1(3)	110.7(3)	110.8
N2–C1–C5	120.0(3)	121.7(3)	120.9
C5–C1–C2	128.9(3)	127.6(3)	128.2
C1–C2–C3	107.1(3)	107.1(3)	106.9
N1–C3–C2	105.0(2)	105.3(3)	105.3
N1–C3–C6	126.7(2)	126.9(3)	127.4
C2–C3–C6	128.2(3)	127.7(3)	127.3
H7–N3–C4–S1	1.6	−1.8	0.7
Cl11–Hg–Cl1–S1	99.7	133.1	127.7
Cl1–Hg–S1–C4	−45.0	4.5	0.4
Hg–Cl1–H7–N3	101.7	122.3	18.0
S1–C4–N1–N2	171.0	−168.7	179.2

[a] For the numbering of atoms see Fig. 3. The numbering of the atoms in **L′** can be derived from that of **L** using the prefix "1" as in the discussion of the crystal structure of the ligand.

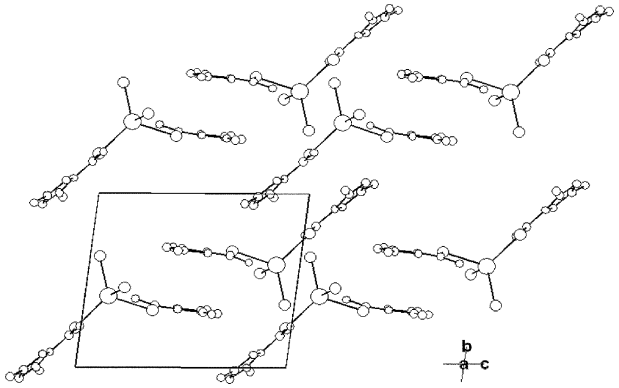

Fig. 4 Packing diagram for HgL_2Cl_2.

agree within experimental error, the two Hg–S bond distances differ by 0.09 Å. Both pyrazole rings are essentially planar, with the largest deviation from planarity being 0.030(3) Å. The plane of the thiocarboxamide group forms a dihedral angle of about 11° with the plane of the pyrazole ring.

The packing diagram for HgL_2Cl_2 is depicted in Fig. 4. It shows that the HgL_2Cl_2 molecules pack with the pyrazole rings parallel but displaced, giving rise to a distance of 3.85 Å between the parallel ring centroids. Hence, there are no significant intermolecular stacking interactions between the HgL_2Cl_2 molecules.

3.3. Theoretical study of the coordination of L to $HgCl_2$

In order to obtain insight into the coordination properties of **L** to $HgCl_2$, we performed quantum chemical calculations on selected structures of HgL_2Cl_2. We probed **L**···$HgCl_2$ interactions with all three donors, *viz.*, the sulfur, the "pyridine" nitrogen N_{py}, and the amino nitrogen atom.§

We started with the optimisation of the asymmetric geometry obtained from the X-ray analysis. The geometry optimisation converged to a symmetric (C_2) structure, keeping the monodentate S-coordination of **L** to Hg, but containing two equivalent Cl···H hydrogen bonds (**1a** in Fig. 5). In the isolated HgL_2Cl_2 molecule the double hydrogen-bonded arrangement seems to be more stable, hence the observed asymmetric molecular geometry with a single Cl···H hydrogen bond in the crystal (*vide supra*), is probably due to packing effects.

Besides **1a**, four additional possible structures were investigated (*cf.* Fig. 5). Structure **1b** (C_s symmetry) contains monodentate S-coordination and differs from **1a** in the relative orientation of the two **L** ligands: whereas in **1a** the **L** ligands orient anti-parallel and their NH_2 hydrogens form hydrogen bonds with different Cl atoms of the $HgCl_2$ moiety, they are parallel in **1b** and the NH_2 hydrogens form contacts with the same Cl atom. Structures **2a** and **2b** are formed by the coordination of N_{py} to Hg and have C_2 and C_s symmetry, respectively. As the ligand **L** may take part in a bidentate coordination [as found in the case of Ni(II), Cu(I,II) and Co(II) complexes[17,18,36]], the probability of a chelate coordination of **L** was investigated in structure **3** possessing C_{2h} symmetry.

The B3LYP/6-31G** calculations gave **1a** as the global minimum on the PES of HgL_2Cl_2. Hence, the preference for S-coordination over N-coordination is not merely the result of packing effects in the solid phase. The stability of the complex is very high: the dissociation energy of **1a** to $HgCl_2$ + 2**L** was computed to be 121.2 kJ mol^{-1}.

The frequency calculations indicated the local minimum character of the N_{py}-coordinated **2a** structure. It is consider-

§ Note that the selected model structures may not cover all the local minima on the potential energy surface (PES) of HgL_2Cl_2. A complete scan of the PES of HgL_2Cl_2 is, however, out of the scope of the present study.

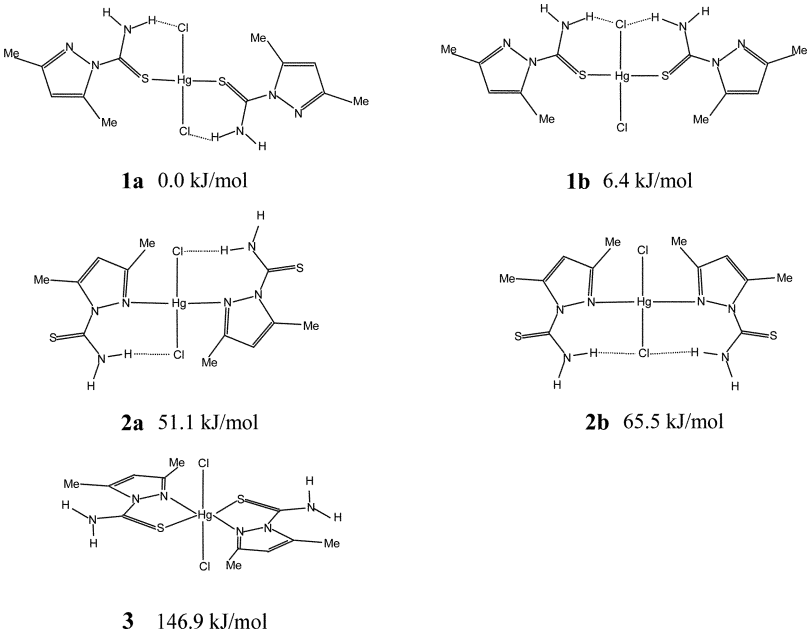

Fig. 5 Relative calculated stabilities for selected models of **L**···Hg coordination.

ably (by 51.1 kJ mol^{-1}) higher in energy than the global minimum **1a**. The structures with parallel orientation of the **L** ligands (**1b** and **2b**) have slightly lower stabilities than the respective C_2 ones (*cf.* Fig. 5) and represent first-order saddle points on the PES. The vibrations with imaginary frequency values indicate a tendency for distortion from the C_s symmetry, probably due to unfavourable steric effects. Slight distortions of **1b** and **2b** result in asymmetric local minimum structures showing only marginal changes in the energy (around 0.3 kJ mol^{-1}) and **L**···$HgCl_2$ distances (around 0.01 Å) with respect to **1b** and **2b**.

The chelate complex **3** lies considerably (146.9 kJ mol^{-1}) higher in energy than the global minimum **1a** and corresponds to a sixth-order saddle point on the PES. Note that four of the imaginary frequencies express the effort of the NH_2 groups to turn from the constrained co-planar position with the ring. A release of this constraint, however, broke the bidentate coordination and the calculations converged to a C_2 saddle point with bifurcated Hg···**L** coordination.

Our calculations using initial structures with H_2N···Hg coordination revealed that the NH_2 nitrogen is not able to participate in any donor-acceptor interaction with Hg in the title complex. The geometric parameters reveal a planar NH_2 group in **L** due to the strong delocalisation of the nitrogen lone pair within the $N_{py}C(S)NH_2$ moiety. Consequently, the NH_2 nitrogen is a very bad electron donor in **L**. On the other hand, the observed hydrogen-bonding interactions of the NH_2 group play a significant role in the stabilisation of the complex structures.

The computed geometric parameters of the global minimum **1a** are given in Table 3, together with the data obtained from the X-ray diffraction analysis. Comparison of the two sets of parameters reveals generally a good agreement for the bond distances and bond angles. Most bond distances agree to within 0.01 Å and bond angles to within 2°. The only considerable differences appear for the HgS_2Cl_2 moiety. The shorter Hg–Cl1 bond distance in the crystal may be attributed to the distortion (breaking of the Cl1···H hydrogen bond) in the solid phase. On the other hand, the calculated Hg–S distances are longer by *ca.* 0.3 Å than those found in the crystal. Considering that donor-acceptor interactions (like Hg···S) are generally weaker than covalent bonds, a large impact of packing effects on the Hg–S distance in the crystal of HgL_2Cl_2 cannot be excluded. In order to assess the usual Hg–S bond distance in Hg···thiocarboxamide complexes we performed a search of the Cambridge Structure Database (CSD).[37] The distribution of the obtained 127 bond lengths found is shown in Fig. 6. The Hg–S distances of 2.486 and 2.575 Å obtained from the X-ray diffraction study of the title compound agree well with the distribution found in the CSD. On the other hand, Hg–S bond distances larger than 2.8 Å are extremely rare in such compounds (only four were found). This suggests an overestimation of the Hg–S bond distance at the computational level employed.

3.4. Factors determining the coordination of L to $HgCl_2$

One of our key aims in the systematic studies of pyrazole type ligands and their coordination is to determine the most important factors that govern the course of complex formation. These factors are diverse and numerous, and include the type and position of the substituents, the basicity of the complexing species, the crystal field stabilisation energy (CFSE), steric requirements of the fragments, bonding preferences of the central metal atom and the interactions of the fragments with the solvent. Regarding the crystal structure of the complexes formed in the solid state, the major factors include the inter- and intramolecular interactions.

The usual coordination mode of pyrazole ligands is coordination through N_{py}. In the absence of a second donor in the ortho position the ligand acts in a monodentate way, as in the

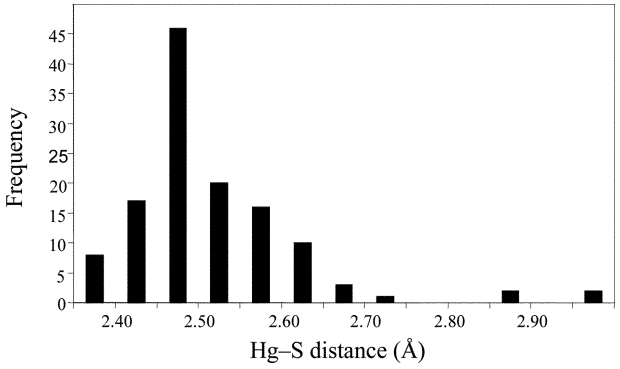

Fig. 6 CSD results on the Hg–S bond in thiocarboxamide complexes.

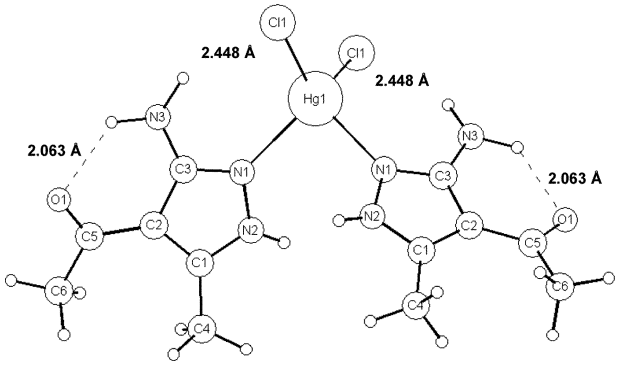

Fig. 7 Molecular structure and intramolecular hydrogen bonding in $HgL^1_2Cl_2$ ($\mathbf{L^1}$ = 3-amino-4-acetyl-5-methylpyrazole).[38]

case of the chemically related $HgL^1{}_2Cl_2$ ($\mathbf{L^1}$ = 3-amino-4-acetyl-5-methylpyrazole) complex.[38] In the crystal of $HgL^1{}_2Cl_2$ two $\mathbf{L^1}$ molecules are coordinated to the central Hg atom through N_{py} in a symmetric fashion (*cf.* Fig. 7). Within $\mathbf{L^1}$ there is a fairly strong intramolecular hydrogen bond between the acetyl oxygen and the amino hydrogen (O···H = 2.063 Å). This strong interaction may primarily determine the orientation of the NH_2 group and allows only a very weak interaction of the other amino hydrogen with the chlorine atom (Cl···H = 2.448 Å).

As mentioned above, **L** has three potential donors: the pyridine and the amino nitrogen atoms and the sulfur atom. In addition, there is a possibility for amino group deprotonation. When the ligand is deprotonated during complex formation, the anions of the metal salt are replaced by the deprotonated ligand anion as in the reaction Ni(II) + **L** = $Ni(L–H)_2$ (L–H = deprotonated **L**) resulting in a square-planar $Ni(L–H)_2$ complex.[17] In contrast, in the reaction of **L** with Cu(II) and Co(II) halides dinuclear $M_2L_2Cl_4$ complexes with the metals in tetrahedral and trigonal bipyramidal coordination, respectively, were formed.[18] In the case of $CuBr_2$, the redox properties of the reactants play also an important role. The reduction of Cu(II) to Cu(I) resulted in the $Cu_2L_2Br_2$ dinuclear complex, which is also sterically advantageous for the large Br ligands. In all the above reactions **L** acts as a bidentate ligand by coordination through both N_{py} and S.

The formation of the title HgL_2Cl_2 complex takes a different course as the coordination is established exclusively through the sulfur atom. This preference for S-coordination is also supported by the reaction of **L** with $HgCl_2$ using a mole ratio of 1 : 1. Instead of the possible monoligand complex with a bidentate coordination of **L** we obtained HgL_2Cl_2. Compared with the Cu(II) and Co(II) complexes, the different complexation of **L** with $HgCl_2$ is in agreement with Pearson's theory.[39–41] Namely, the soft acid Hg(II) prefers a reaction with the soft base sulfur instead of the harder base N_{py}. A similar coordination of Hg(II) to sulfur (instead of N) was also found in its complex with 1,3-thiazolidine-2-thione.[42] In contrast, the somewhat harder acids Cu(II) and Co(II) are better suited to bind to the harder base N_{py}.

Another important factor for **L**···$HgCl_2$ coordination may be the larger size of Hg compared to the first-row transition metal elements Cu and Co. The larger size allows a less strained arrangement of two **L** ligands around the metal center, thus a mononuclear complex (instead of dinuclear like in the cases of Cu and Co) can be formed. The steric conditions favour the S-monocoordination over the more crowded N_{py}-coordination (*cf.* Fig. 5). The structure is further stabilised by Cl···H hydrogen bonds, also contributing to the preference of structure **1a** over **2a**. The hydrogen bonds are calculated to be much weaker in **2a** (*cf.* Table 4), because these NH_2 hydrogens are involved in bifurcated hydrogen bonding with N_{py}. In addition to the generally lower stability of the **1b** and **2b** structures compared to **1a** and **2a**, respectively, we observed somewhat longer Hg···S, Hg···N_{py} and Cl···H distances (hence weaker interactions) in the former structures.

Table 4 Distances (Å) characterising the donor-acceptor and hydrogen-bonding interactions in the structures **1a**, **1b**, **2a**, **2b** and **3** from B3LYP/6-31G** computations

Parameter	1a	1b	2a	2b	3
Hg–S	2.831	2.843	—	—	3.098
Hg–N_{py}	—	—	2.596	2.743	2.775
Cl···H	2.197	2.225	2.474	2.557	—
N_{py}···H	2.057	2.058	2.440	2.285	—

The low stability and saddle-point character of structure **3** is in agreement with the usual preference of Hg(II) complexes for tetrahedral coordination. This preference is illustrated by the distribution of the X–Hg–X (X = any atom) angles shown in Fig. 8 from our CSD[37] search on tetracoordinated Hg (851 hits).

3.5. FT-IR spectra

The FT-IR spectrum of solid HgL_2Cl_2 is depicted in Fig. 9, whereas the assignment of the absorption bands is given in Table 5. The assignment was performed on the basis of our recent normal coordinate analysis results (using a scaled quantum mechanical force field from DFT calculations) on **L**.[43] We found a very good agreement between the experimental frequencies of solid **L** and those of HgL_2Cl_2 with an average deviation of 10.1 cm^{-1}. Obviously, the coordination of Hg to the terminal S atom can exert only a minor influence on the vibrations of the pyrazole ring. A major part of the deviations may originate from the different intermolecular interactions in the crystals of **L** and HgL_2Cl_2. A perceptible effect of complex formation can be expected only for the vibrations of the CS group. The CS asymmetric stretch is the dominant vibration in the ν_{23} fundamental; however, the CS vibrations generally appear to be strongly mixed in several other fundamentals. Hence the only effect in the IR spectrum that could be attributed to complex formation is the 9 cm^{-1} decrease of the wavenumber of ν_{23} in HgL_2Cl_2 with respect to **L**.

The assignment of the FT-IR spectra of HgL_2Cl_2 was further supported by the present B3LYP/6-31G** calculations (*cf.* Table 5). The average deviation between the experimental and the unscaled B3LYP/6-31G** frequencies was 45 cm^{-1}, excluding the two NH_2 stretching modes, which are affected strongly by the different hydrogen-bonding patterns of the free molecule and in the crystal. The computations also facilitated

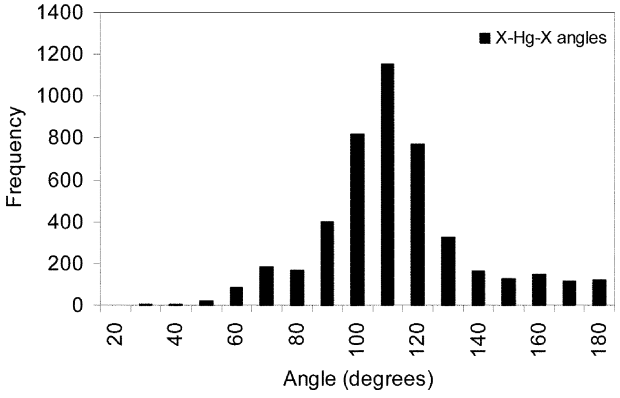

Fig. 8 X–Hg–X (X = any atom) angles for tetracoordinated Hg complexes.

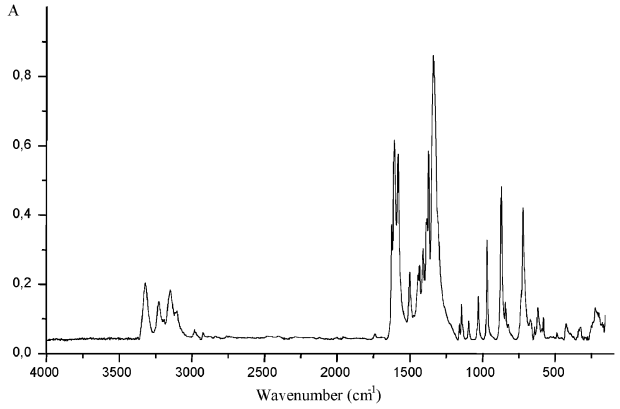

Fig. 9 FT-IR spectrum of solid HgL_2Cl_2.

the identification of the HgS_2 and $HgCl_2$ stretching bands in the FT-IR spectrum. The bands at 330 and 300 cm^{-1} assigned to the asymmetric and symmetric HgS_2 stretching vibrations, respectively, fall in the range of 290–350 cm^{-1} reported for various M···S complexes (M = Pt, Ir with Me_2S and Et_2S ligands).[36] These fundamentals contain a considerable amount of in-plane C–CH_3 bending, which is the major contribution to the 330 cm^{-1} fundamental.

Contrary to the HgS_2 vibrations, both the symmetric and asymmetric $HgCl_2$ stretchings are essentially pure in their fundamentals. The very intense asymmetric $HgCl_2$ stretching can be assigned to the strong band at 226 cm^{-1} in the far-IR spectrum of HgL_2Cl_2, whereas the weaker band of the symmetric $HgCl_2$ stretching is probably hidden by the intense absorption of ν_{37}.

It is known that the MX (M = heavy transition metal, X = halogen) stretching vibrations are very sensitive to the structure of the complex. The M–Cl stretching vibrations appear generally in the range of 400–200 cm^{-1}. The HgL_2Cl_2 complex has a distorted tetrahedral structure, whereas in the literature we found far-IR data on square-planar and octahedral ML_2Cl_2 complexes only. The $PtCl_2$ stretching vibrations in such complexes were reported to appear around 330 cm^{-1},[36] hence higher by *ca.* 100 cm^{-1} than the present values for HgL_2Cl_2. Note that the strong intramolecular hydrogen bond found in the HgL_2Cl_2 complex may also result in some red-shift of the $HgCl_2$ stretching frequencies.

Table 5 Observed and calculated fundamentals (cm^{-1}) of HgL_2Cl_2

ν	Exptal[a]	Calcd[b]	Assignment[c]
1	3320 w	3585 (599)	$\nu_{as}NH_2$
2	3149 m, 3228 m	3327 (1534)	$\nu_{s}NH_2$
3	3102 sh	3271 (2)	νCH_{ring}
4	2983 w	3142 (52)	$\nu_{as}CH_3$
5	2973 sh	3110 (22)	$\nu_{as}CH_3$
6	2923 w	3053 (41)	$\nu_{s}CH_3$
7	1607 s, 1625 m	1664 (39)	βNH_2, νring
8	1581 s	1638 (296)	βNH_2, νring
9	1501 m	1552 (49)	νring,
10	1443 m	1502 (83)	$\delta_{as}CH_3$
11	1434 m	1494 (37)	$\delta_{as}CH_3$
12	1409 m	1477 (5)	νring, $\delta_{as}CH_3$, βNH_2
13	1387 m	1458 (116)	νring, $\delta_{s}CH_3$
14	1383 m	1434 (50)	$\delta_{s}CH_3$
15	1372 s	1419 (128)	$\delta_{s}CH_3$
16	1338 s	1374 (1390)	νN_{ring}–C, $\delta_{r}NH_2$
17	1159 w	1192 (1)	βCH_{ring}
18	1146 w	1189 (15)	βCH_{ring}, $\delta_{r}NH_2$,
19	1095 w	1134 (45)	νring
20	1039 sh	1068 (6)	$\delta_{r}CH_3$
21	1029 m	1057 (30)	$\delta_{r}CH_3$, βring
22	969 m	995 (81)	νring, $\delta_{r}CH_3$
23	871 m	905 (237)	νCS, $\delta_{r}NH_2$
24	823 w	826 (33)	γCH_{ring}
25	733 sh	755 (28)	γNH_2
26	722 s	737 (96)	νC–CH_3, βring,
27	671 m	682 (241)	γNH_2
28	641 w	672 (9)	τring,
29	621 w	645 (28)	τring, τNH_2
30	590 w	629 (26)	βring, νN_{ring}–C, βCS
31	581 w	588 (12)	νC–CH_3, βring
32	493 w	504 (3)	βC–CH_3, βCS
33	429 w	447 (52)	βC–NH_2
34	330 m	322 (16)	βC–CH_3, $\nu_{s}HgS_2$
35	300 w	322 (5)	ν_{as}Hg–S, βC–CH_3
36	226 s	261 (48)	$\nu_{as}HgCl_2$
37	206 sh	235 (27)	βC–NH_2, βC–CH_3
38	~200[d]	238 (17)	$\nu_{s}HgCl_2$
39	174 w	177 (2)	γC–CH_3
40	160 w	146 (4)	γC–NH_2, γC–CH_3
41		121 (22)	γHgCl

[a] FT-IR data obtained from a solid sample. The abbreviations s, m, w, sh mean strong, medium, weak, shoulder, respectively. [b] Calculated at the B3LYP/6-31G** level. IR intensities are given in parenthesis (km mol^{-1}). [c] Main components in the normal modes: ν= strech (s: symmetric, as: asymmetric); β = bend; δ = deformation; γ = out-of-plane bend; τ = torsion. [d] Hidden.

3.6. Thermal decomposition of L and HgL_2Cl_2

The thermal decomposition of **L** starts at 370 K and occurs continuously in argon, without any clearly distinguishable decomposition steps. The decomposition is finished at 1000 K without residue. In air, some oxidation processes take place. The DSC curve shows the melting of the compound with an onset temperature of 360 K, suggesting that the melting is accompanied with an endothermic decomposition.

As expected, the thermal stability of the complex is somewhat higher than that of the ligand. The decomposition takes place in three steps, starting at 400 K. The first step probably represents loss of a ligand molecule, accompanied with its fragmentation and the evaporation of an HCl molecule. The next decomposition step starts above 565 K; it involves the evaporation of the second ligand fragment and probably a fraction of Hg (in the form of a non-identified compound), with a DTG minimum at 710 K. The process is finished at about 800 K with a coke residue of 8%. The endothermic decomposition is accompanied with the melting of the sample at 400 K. The decomposition patterns in air and argon are very similar.

4. Conclusions

In the present study, a joint experimental and theoretical analysis of the HgL_2Cl_2 complex has been performed. We determined the molecular geometry in both the crystal and the gas phase, using single crystal X-ray diffraction and quantum chemical computations, respectively. The Hg atom is in a distorted tetrahedral coordination, bonded to two Cl atoms and two thiocarboxamide S atoms. The main difference appears in the breaking of C_2 symmetry and one of the Cl···H hydrogen bonds in the solid phase, presumably due to the effect of neighbours.

The Hg–S bond distance is around 2.5 Å, which is about the same as the sum of the covalent radii of the two atoms. The strong bond is manifested in the large (121.2 kJ mol^{-1}) dissociation energy to $HgCl_2$ + 2**L**. Besides the donor-acceptor bonding, the Cl···H hydrogen bonds contribute considerably to the stability of the complex. The length of the hydrogen bond is 2.2 Å, characteristic of medium-strength interactions.

Our quantum chemical calculations justified the preference of the monodentate S-coordination of **L** to Hg, where the two **L** ligands are arranged anti-parallel with respect to each other.

The structure with the parallel **L** arrangement lies slightly higher in energy (6 kJ mol^{-1}), whereas the monodentate N_{py}-coordination lies considerably (51 kJ mol^{-1}) higher in energy. Due to large steric effects, the bidentate chelate arrangement is not a reasonable structure on the potential energy surface.

The preference of S- over N_{py}-coordination in the global minimum **1a** is the result of complex bonding interactions. According to Pearson's theory, the electronic factor is the soft acid character of Hg(II), which favours a reaction with the soft base sulfur over the medium hard base N_{py}. The S-coordinated structure is further stabilised by the stronger Cl···H hydrogen bonds. From a steric point of view, the coordination through the N_{py}, shielded by the neighbouring methyl and thiocarboxamide groups, is less advantageous in the mononuclear HgL_2Cl_2 complex.

In addition to the structural characteristics, we determined the vibrational properties of HgL_2Cl_2 by a joint FT-IR and theoretical analysis. On the basis of the computations, the HgS_2 stretching vibrations have been assigned to bands at 330 and 300 cm^{-1}, whereas the asymmetric $HgCl_2$ stretching mode corresponds to the band at 226 cm^{-1} in the far-IR spectrum.

The X-ray diffraction analysis of the ligand **L** revealed the presence of an asymmetric unit containing two independent molecules with very similar geometric parameters. In the crystal **L** forms $R_2^2(8)$ centrosymmetric dimers, which are connected to two additional molecules by S···H hydrogen bonds.

Acknowledgements

Financial support from the Hungarian Scientific Research Foundation (OTKA No T038189) and computational time from the National Information Infrastructure Development Program of Hungary is gratefully acknowledged. A. K. thanks the Bolyai Foundation for support. M. Sz. K. would like also to thank the Domus Hungarica Scientiarum Artiumque Foundation for their support. The work was financed in part by the Ministry for Science and Environmental protection of the Republic of Serbia (Grant No 1318). Z. K. Jaćimović thanks the Austrian Ministry of Education, Science and Culture for support and the Institut für Mineralogie und Kristallographie (University of Vienna) and Univ. Prof. Dr Ekkehart Tillmanns.

References

1 Ž. K. Jaćimović, I. Radosavljević Evans, J. A. K. Howard, K. Mészáros Szécsényi and V. M. Leovac, *Acta Crystallogr., Sect C*, 2004, **60**, m467.
2 (*a*) P. Rauter, J. A. Figueiredo, M. I. Ismael and J. Justino, *J. Carbohydr. Chem*., 2004, **23**, 513; (*b*) R. Sridhar, P. T. Perumal, S. Etti, G. Shanmugam, M. N. Ponnuswamy, V. R. Prabavathy and N. Mathivanan, *Bioorg. Med. Chem. Lett*., 2004, **14**, 6035; (*c*) A. K. Jain, S. M. Moore, K. Yamaguchi, T. E. Eling and S. J. Baek, *J. Pharmacol. Exp. Ther*., 2004, **311**, 885.
3 (*a*) W. G. Haanstra, *Ph.D. Thesis*, Leiden University, Leiden, The Netherlands, 1991; (*b*) W. G. Haanstra, W. A. J. W. van der Donk, W. L. Dreissen, J. Reedijk, J. S. Wood and M. G. B. Drew, *J. Chem. Soc., Dalton Trans*., 1990, 3123.
4 E. I. Solomon, U. M. Sundaram and T. E. Machonkin, *Chem. Rev*., 1996, **96**, 2563.
5 P. Gamez, J. von Harras, O. Roubeau, W. L. Driessen and J. Reedijk, *Inorg. Chim. Acta*, 2001, **324**, 27.
6 J. E. Cosgriff and G. B. Deacon, *Angew. Chem., Int. Ed*., 1998, **37**, 286.
7 E. C. Plappert, T. Stumm, H. van der Bergh, R. Hauert and K.-H. Dahmen, *Chem. Vap. Deposition*, 1997, **3**, 37.
8 C. Pettinari, F. Marchetti, C. Santini, R. Pettinari, A. Drozdov, S. Troyanov, G. A. Battiston and R. Gerbasi, *Inorg. Chim. Acta*, 2001, **315**, 88.
9 S. Trofimenko, *Prog. Inorg. Chem*., 1986, **34**, 115.
10 N. T. Sorrel, *Tetrahedron*, 1989, **45**, 3.
11 S. Trofimenko, *Chem. Rev*., 1993, **93**, 943.
12 R. Mukherjee, *Coord. Chem. Rev*., 2000, **203**, 151.
13 K. Mészáros Szécsényi, V. M. Leovac, V. I. Češljević, A. Kovács, G. Pokol, Gy. Argay, A. Kálmán, G. A. Bogdanović, Ž. K. Jaćimović and A. Spasojević-de Biré, *Inorg. Chim. Acta*, 2003, **353**, 253.
14 K. Mészáros Szécsényi, E. Z. Ivegeš, V. M. Leovac, Lj. S. Vojinović, A. Kovács, G. Pokol, J. Madarász and Ž. K. Jaćimović, *Thermochim. Acta*, 1998, **316**, 79.
15 K. Mészáros Szécsényi, E. Z. Ivegeš, V. M. Leovac, A. Kovács, G. Pokol and Ž. K. Jaćimović, *J. Therm. Anal. Calorim*., 1999, **56**, 493.
16 K. Mészáros Szécsényi, V. M. Leovac, Ž. K. Jaćimović, V. I. Češljević, A. Kovács and G. Pokol, *J. Therm. Anal. Calorim*., 2001, **63**, 723.
17 I. Radosavljević Evans, J. A. K. Howard, K. Mészáros Szécsényi, V. M. Leovac and Ž. K. Jaćimović, *J. Coord. Chem*., 2004, **57**, 469.
18 I. Radosavljević Evans, J. A. K. Howard, L. E. M. Howard, J. S. O. Evans, Ž. K. Jaćimović, V. S. Jevtović and V. M. Leovac, *Inorg. Chim. Acta*, 2004, **357**, 4528.
19 K. Mészáros Szécsényi, V. M. Leovac, Ž. K. Jaćimović and G. Pokol, *J. Therm. Anal. Calorim*., 2003, **74**, 943.
20 W. Kaim and B. Schwederski, *Bioinorganic Chemistry, Inorganic Elements in the Chemistry of Life: An Introduction and Guide*, Wiley, Chichester, 1994.
21 A. Altomare, G. Cascarano, C. Giacovazzo, A. Guagliardi, M. C. Burla, G. Polidori and M. Camalli, *J. Appl. Crystallogr*., 1994, **27**, 435.
22 G. M. Sheldrick, *SHELXL-97, Program for refinement of crystal structures*, University of Göttingen, Germany, 1997.
23 A. L. Spek, *PLATON-99, Molecular Geometry Program*, University of Utrecht, The Netherlands, 1999.
24 *SAINT*, Release 6.22., Bruker Analytical Systems, Madison, WI, USA, 1997–2001.
25 G. M. Sheldrick, *SADABS*, University of Göttingen, Germany, 1998.
26 P. W. Betteridge, J. R. Carruthers, R. I. Cooper, K. Prout and D. J. Watkin, *J. Appl. Crystallogr*., 2003, **36**, 1487.
27 M. J. Frisch, G. W. Trucks, H. B. Schlegel, G. E. Scuseria, M. A. Robb, J. R. Cheeseman, V. G. Zakrzewski, J. A. Montgomery, Jr., R. E. Stratmann, J. C. Burant, S. Dapprich, J. M. Millam, A. D. Daniels, K. N. Kudin, M. C. Strain, O. Farkas, J. Tomasi, V. Barone, M. Cossi, R. Cammi, B. Mennucci, C. Pomelli, C. Adamo, S. Clifford, J. Ochterski, G. A. Petersson, P. Y. Ayala, Q. Cui, K. Morokuma, D. K. Malick, A. D. Rabuck, K. Raghavachari, J. B. Foresman, J. Cioslowski, J. V. Ortiz, A. G. Baboul, B. B. Stefanov, G. Liu, A. Liashenko, P. Piskorz, I. Komaromi, R. Gomperts, R. L. Martin, D. J. Fox, T. Keith, M. A. Al-Laham, C. Y. Peng, A. Nanayakkara, C. Gonzalez, M. Challacombe, P. M. W. Gill, B. G. Johnson, W. Chen, M. W. Wong, J. L. Andres, M. Head-Gordon, E. S. Replogle and J. A. Pople, *GAUSSIAN 98 (Revision A.9)*, Gaussian, Inc., Pittsburgh, PA, 1998.
28 A. D. Becke, *J. Chem. Phys*., 1993, **98**, 5648.
29 C. Lee, W. Yang and R. G. Parr, *Phys. Rev. B*, 1988, **41**, 785.
30 P. J. Hay and W. R. Wadt, *J. Chem. Phys*., 1985, **82**, 270.
31 A. W. Ehlers, M. Böhme, S. Dapprich, A. Gobbi, A. Höllwarth, V. Jonas, K. F. Köhler, R. Stegmann, A. Veldkamp and G. Frenking, *Chem. Phys. Lett*., 1993, **208**, 111.
32 S. F. Boys and F. Bernardi, *Mol. Phys*., 1970, **19**, 553.
33 A. L. Lamas-Saiz, C. Foces-Foces, I. Sobrados, N. Jagerovic and J. Elguero, *J. Mol. Struct*., 1999, **478**, 81.
34 T. Latour and S. E. Rasmussen, *Acta Chem. Scand*., 1973, **27**, 1845.
35 L. Shimoni, J. P. Glusker and C. W. Bock, *J. Phys. Chem*., 1996, **100**, 2957.
36 K. Nakamoto, *Infrared and Raman Spectra of Inorganic and Coordination Compounds. Part B: Applications in Coordination Organometallic and Bioinorganic Chemistry*, Wiley, New York, 1997, pp. 184, 186 and 204.
37 F. H. Allen, *Acta Crystallogr., Sect. B*, 2002, **58**, 380.
38 A. Hergold-Brundić, B. Kaitner, B. Kamenar, V. M. Leovac, E. Z. Ivegeš and N. Juranić, *Inorg. Chim. Acta*, 1991, **188**, 151.
39 R. G. Pearson, *J. Am. Chem. Soc*., 1963, **85**, 3533.
40 R. G. Pearson and J. Songstad, *J. Am. Chem. Soc*., 1967, **89**, 1827.
41 T.-L. Ho, *Chem. Rev*., 1975, **75**, 1.
42 Z. Popović, G. Pavlović, Ž. Soldin, J. Popović, D. Matković-Čalogović and M. Rajić, *Struct. Chem*., 2002, **13**, 4.
43 D. Nemcsok and A. Kovács, in preparation.